

# Fibre Type Identification based on Power Profile Estimation

Motohiko Eto, Kazuyuki Tajima, Kyousuke Sone, Setsuo Yoshida, Ryu Shinzaki, Shoichiro Oda, and Takeshi Hoshida

Fujitsu Limited, Kawasaki, Japan, [eto.motohiko@fujitsu.com](mailto:eto.motohiko@fujitsu.com)

**Abstract** We developed a technique to identify fibre type based on power profile estimation using coherent receivers. With the proposed method, SSMF and NZ-DSF were successfully identified in 96GBd DP-16QAM signal, 9-span transmission testbed. ©2023 The Author(s)

## Introduction

Nowadays, to cope with increasing demand for network traffic economically, improvement of accuracy in design of optical network is inevitable [1]. In such network design, fibre type identification has a critical role, because fibre type is one of essential physical parameters and possibly causes degradation of transmission capability in case of mismatch from network design [2] due to an unexpected error in network management and operation. Therefore, the realization of fibre type identification in reasonable costs highly demanded to maximize the network capacity. As a prior work [3], the mixed integer linear program was applied to provide the functionality. Although this has the advantage of using chromatic dispersion measured by widely used coherent receivers, it might be difficult to utilize it in the early stage of network where the wavelength usage is low.

Recently we experimentally demonstrated the fibre type identification based on a longitudinal optical power profile estimation (PPE) [4] using the software prototype [5], which is free from the above limitation of wavelength usage. In this paper, we extend it by adding the experimental evaluation under various conditions in 96 Gbaud (GBd) dual-polarization 16-quadrature amplitude modulation (DP-16QAM) signal, 9-span transmission testbed and the proposal of novel dispersion slope estimation, which is the

advantage compared with the conventional OTDR-based measurement, the machine-learning-based method [6], and minimum-mean-square-error (MMSE)-based PPE method [7]. Since this enables to identify more fibre types by using only waveform data measured by a coherent receiver, we believe our proposal can support operators network design optimization and efficient operation.

## Method

Fig.1 illustrates the functional block diagram and flowchart of our method for fibre type identification based on Rx-side DSP algorithm [5]. First, a PPE processed along steps described in Fig.1(a). A digital coherent receiver at the end of link converts the received signal into the electromagnetic fields, and calculate CD compensation (CDC), nonlinear compensation (NLC), and residual CDC. The outcome and the reference signal, which is generated from waveform reconstruction are calculated to evaluate a correlation between the two. By sweeping the amount of CDC, we obtain the estimated power profile along the CD. The calculated power profile is input into the processing for fibre type identification, described in Fig. 1(b). In the next step, to estimate the CD of each span, we detect the peaks from the estimated power profile. Then, the CD coefficient is derived from estimated CD and the fibre length

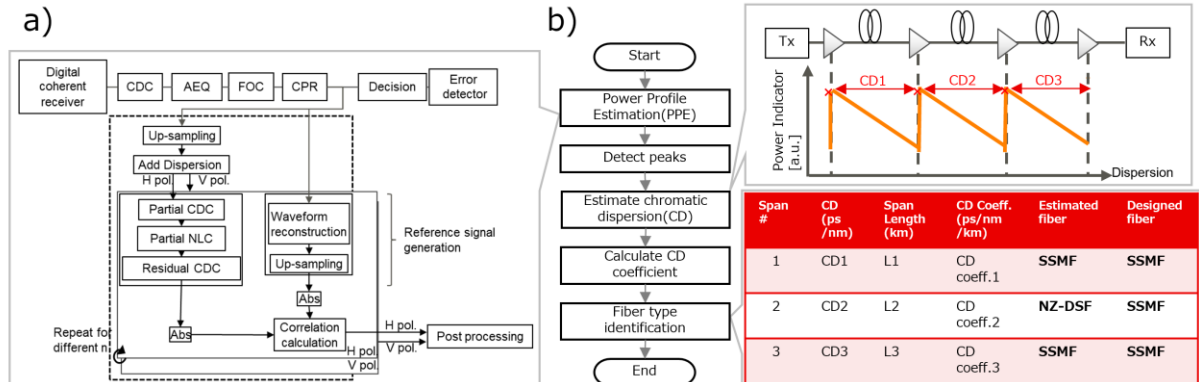


**Fig. 1:** (a) Block diagram of PPE, CDC: Chromatic dispersion compensation, AEQ: Adaptive equalizer, FOC: Frequency offset compensator, CPR: Carrier phase recovery, (b) Flowchart of fibre type identification.

of each span, which is provided as data for optical network design. After that, we identify fibre type of each span by referencing a list of CD coefficients corresponding to expected fibre types for the link. The information about a different fibre type from the network design can be used to maximize network capacity. In addition, as mentioned above, by calculating several CD coefficients with different central frequencies, we can estimate CD slope of each span, which can be used to identify more fibre types.

### Experimental evaluation

We experimentally verified the proposed method with 640km-long-DWDM transmission line shown in Fig. 2 (a). 96 GBd DP-16QAM signal was used for the measured signal. The central

frequency was set to 193.2 THz. Other neighbouring 44 channels with 100-GHz spacing were generated from amplified spontaneous emission (ASE) source and WSS. The WDM signals were launched into 640-km-long straight line consisting of 9 spans with standard SMF (SSMF) in which the first five spans and last four spans were 80 and 60 km, respectively. To evaluate whether our proposal can identify between SSMF and non-zero DSF (NZ-DSF), we inserted 70 or 75 km NZ-DSF, instead of SSMF into single or multiple span(s) in this transmission line with various combinations shown in Fig. 2 (b) and (c). In the receiver side, after the coherent detection, the data is sampled by digital storage oscilloscope (DSO) at 160 GSa/s and then processed with conventional off-line based digital signal processing (DSP). The demodulated

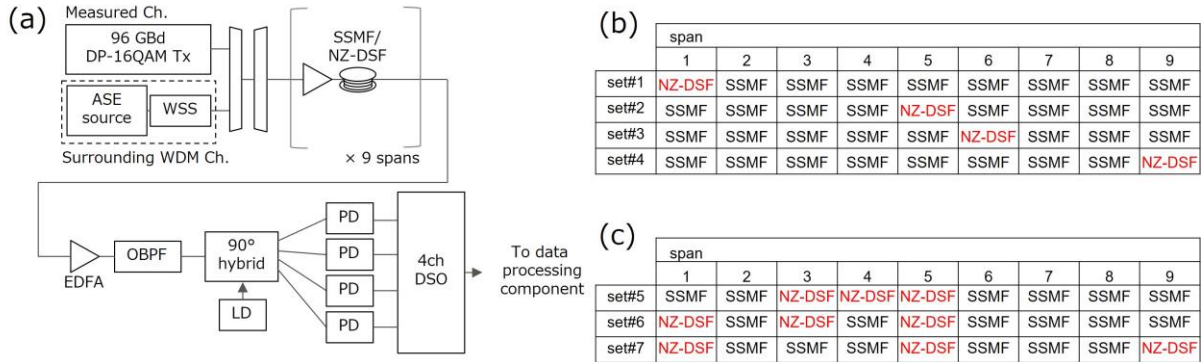


**Fig. 2:** (a) Experimental setup. ASE: Amplified spontaneous emission, WSS: Wavelength selective switch, EDFA: Erbium doped fibre amplifier, OBPF: Optical bandpass filter, PD: Photodiode, LD: Laser diode, DSO: Digital storage oscilloscope.

(b) Experimental sets of fibre combination for the case that single NZ-DSF span was inserted and (c) experimental sets for multiple spans.

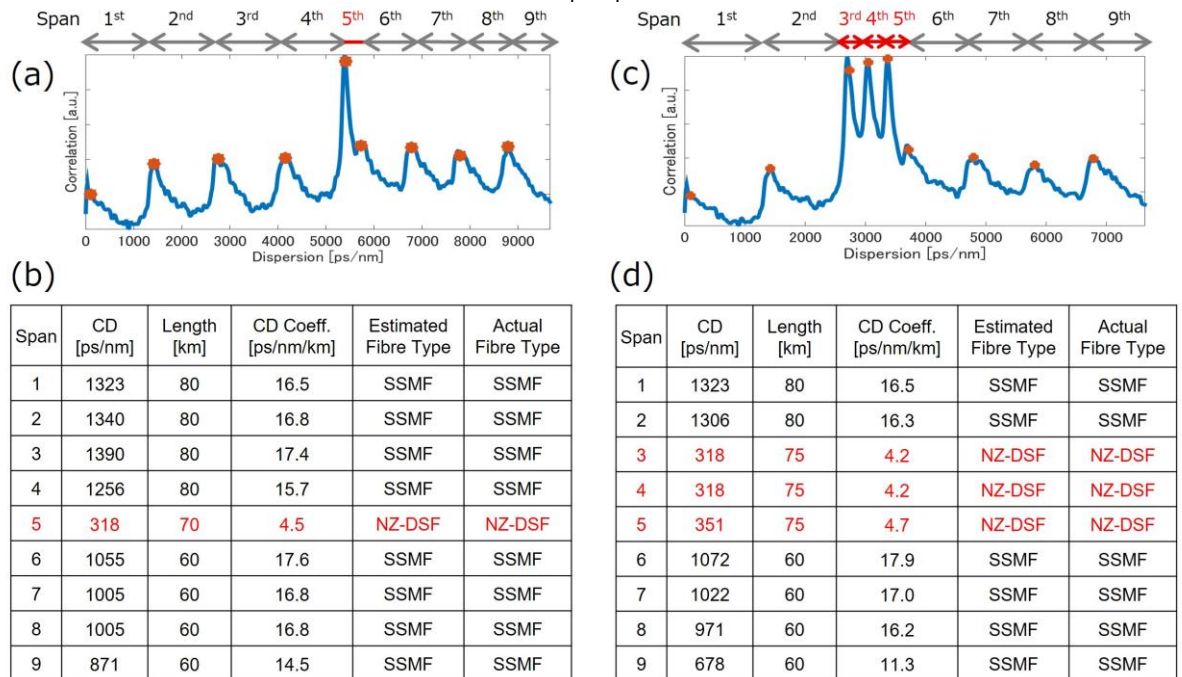


**Fig. 3:** Results for the transmission line includes single NZ-DSF at 5th span as set #2 (a) power profile with detected peaks (b) calculated CD, CD coefficient, and estimated fibre type for each span. (c) and (d) are the results for multiple NZ-DSFs at 3rd, 4th, and 5th span as set #5.

signal data after the carrier recovery process was sent to the flow chart in Fig. 1(b). For the estimation of CD slope, we repeated the measurement with changing the central frequency from 191.8 to 194.9 THz. The blue line and the red symbols in Fig. 3(a) show the calculated power profile and the detected peaks, respectively for the case that NZ-DSF was inserted to 5th span as set #2. Fig. 3(b) summarizes the results of fibre type identification. We can see that for each span, CD coefficient was calculated precisely enough to identify the fibre type between SSMF and NZ-DSF by comparing with a list of CD coefficients where CDs of SSMF and NZ-DSF were defined as between 13.4 and 18.2 ps/nm/km and 2.9 and 6.3 ps/nm/km, respectively following G.652.D and G.655.D. We then discuss the results when multiple NZ-DSFs were inserted to 3rd, 4th, and 5th span as set #5 (Fig. 3(c) and (d)).

Although the relatively small dispersion fibres were concatenated, our method successfully identify the fibre type. To further investigation, we

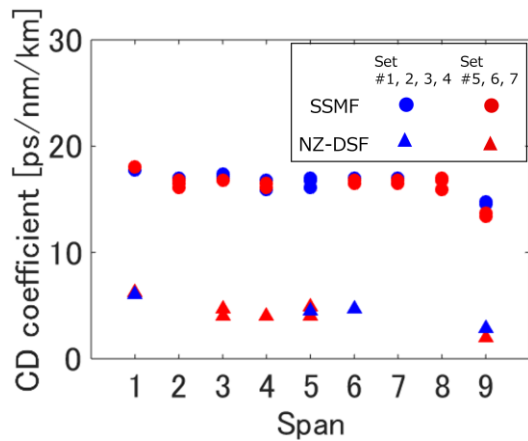


**Fig. 4:** CD coefficients for each span with single NZ-DSF span and multiple NZ-DSF spans. Comparison of CD coefficients for all experiments.

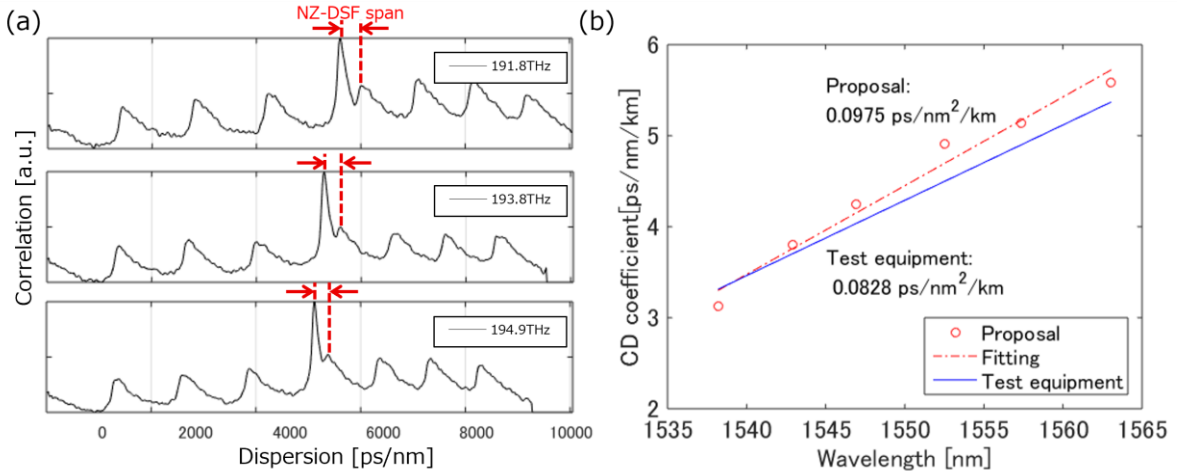


**Fig. 5:** (a) Power profiles measured at 191.8, 193.8 and 194.9THz. (b) CD coefficients and slopes of NZ-DSF at 5th span, obtained by the proposal and the test equipment (Agilent 86038B).

evaluated various combination of location and number of NZ-DSF spans, shown in Fig. 4 illustrating the calculated CD coefficients for SSMF and NZ-DSF versus the span. We confirmed that regardless of location and number of span(s), SSMF and NZ-DSF can be identified with difference between CD coefficients by this method.

We finally demonstrated the estimation of CD slope of NZ-DSF. Fig. 5(a) illustrates the power profiles measured at 191.8, 193.8 and 194.9 THz under the set #2. It is observed that the positions of peak and the duration of peaks were varied with the central frequency. The calculated CD coefficients of NZ-DSF at 5th span were plotted in Fig. 5(b). We compared its accuracy with commercially available test equipment (Agilent 86038B). The resultant CD slopes of the proposal and the equipment were 0.0975 and 0.0828 ps/nm<sup>2</sup>/km, respectively. We believe that the accuracy within 18% error is enough to identify the reduced slope type of NZ-DSF having the slope  $\sim 0.05$  ps/nm<sup>2</sup>/km, e.g. [8].

## Conclusions

We have described the proposed fibre type identification method based on power profile estimation. We experimentally verified that the proposed method could identify SSMF and NZ-DSF regardless of location and number of NZ-DSF span and demonstrated the accurate estimation of CD slope within 18% error.

## Acknowledgements

This work was partly supported by the New Energy and Industrial Technology Development Organization (NEDO), Japan, project, JPNP20017 and by the National Institute of Information and Communications Technology (NICT), Japan, Grant Number 20501.

## References

- [1] Y. Pointurier, "Design of low-margin optical networks," in *Journal of Optical Communications and Networking*, vol. 9, no. 1, pp. A9-A17, Jan. 2017, doi: 10.1364/JOCN.9.0000A9.
- [2] S. J. Savory, "Congestion Aware Routing in Nonlinear Elastic Optical Networks," in *IEEE Photonics Technology Letters*, vol. 26, no. 10, pp. 1057-1060, May15, 2014, doi: 10.1109/LPT.2014.2314438.
- [3] E. Seve, S. Bigo and P. Layec, "Fibre Type Identification: Alleviating Ambiguities," *2022 European Conference on Optical Communication (ECOC)*, Basel, Switzerland, 2022, pp. 1-4.
- [4] T. Tanimura, K. Tajima, S. Yoshida, S. Oda and T. Hoshida, "Experimental demonstration of a coherent receiver that visualizes longitudinal signal power profile over multiple spans out of its incoming signal," *45th European Conference on Optical Communication (ECOC 2019)*, Dublin, Ireland, 2019, pp. 1-4, doi: 10.1049/cp.2019.1031.
- [5] R. Shinzaki, M. Eto, K. Tajima, K. Sone, S. Yoshida, S. Oda, I. Kim, O. Vassilieva, P. Palacharla and T. Hoshida, "Optical Network Tomography: Demonstration of Anomaly Loss Monitoring and Fiber-Type Identification," *2023 Optical Fiber Communications Conference and Exhibition (OFC)*, San Diego, CA, USA, 2023, pp. 1-3.
- [6] T. Sasai *et al.*, "Simultaneous Detection of Anomaly Points and Fiber Types in Multi-Span Transmission Links Only by Receiver-Side Digital Signal Processing," *2020 Optical Fiber Communications Conference and Exhibition (OFC)*, San Diego, CA, USA, 2020, pp. 1-3.
- [7] D. W. Boertjes, M. Reimer and D. Cote, "Practical considerations for near-zero margin network design and deployment [Invited]," in *Journal of Optical Communications and Networking*, vol. 11, no. 9, pp. C25-C34, September 2019, doi: 10.1364/JOCN.11.000C25.
- [8] <https://fiber-optic-catalog.ofsoptics.com/documents/pdf/TrueWaveRSLWP-120-web.pdf>